

NUMERICAL INVESTIGATION OF FORCE TRANSMISSION IN GRANULAR MEDIA USING DISCRETE ELEMENT METHOD

Thong Chung Nguyen¹, Lu Minh Le¹, Hai-Bang Ly², Tien-Thinh Le^{3,*}

¹*Vietnam National University of Agriculture, Hanoi, Vietnam*

²*University of Transport Technology, Hanoi, Vietnam*

³*Duy Tan University, Da Nang, Vietnam*

*E-mail: letienthinh@duytan.edu.vn

Received: 19 January 2020 / Published online: 10 May 2020

Abstract. In this paper, a numerical Discrete Element Method (DEM) model was calibrated to investigate the transmission of force in granular media. To this aim, DEM simulation was performed for reproducing the behavior of a given granular material under uniform compression. The DEM model was validated by comparing the obtained shear stress/normal stress ratio with results published in the available literature. The network of contact forces was then computed, showing the arrangement of the material microstructure under applied loading. The number and distribution of the contacts force were also examined statistically, showing that the macroscopic behavior of the granular medium highly depended on the force chain network. The DEM model could be useful in exploring the mechanical response of granular materials under different loadings and boundary conditions.

Keywords: granular mechanics, discrete element method, force chain, compression test.

1. INTRODUCTION

A granular medium is composed of separate particles that move without dependence and interact with other particles via contact points [1]. Typical granular materials could be found in civil engineering, such as geotechnical engineering, mining or energy production, chemical, pharmaceutical, and agricultural industries [2–4]. Research and development of machinery/device for processing granular materials have been considerably increased over the past ten years, requiring above all a good knowledge of interactions between particulate systems itself and with machine parts [5]. For instance, the coefficient of friction has been introduced, measured to characterize the dissipation of energy when the particles collide [6]. These particulate interactions have been investigated for many years using analytical, semi-analytical, or experimental approaches [3,7,8]. Despite all the efforts, it is not always possible to carry out a large number of configurations

taking into account all the possible parameters [6]. Moreover, experimental works might not have the required ability to investigate the local interactions, particularly in terms of transmission of stress, collapse of force chain under deformation and so on [9]. It clearly showed that a more robust manner is thus required for better understanding and characterizing the mechanical properties of granular materials [10].

From a numerical simulation point of view, the mechanics of granular media can be modeled by either continuum [11–13] or discrete [14–16] approaches. More precisely, in a discrete approach, the Discrete Element Method (DEM) has been primarily employed to simulate granular materials [10, 17]. As an example, Than et al. [18] have developed a DEM model for investigating the plastic response of wet granular material under compression. Also, based on DEM technique, Xie et al. [19] have pointed out the influence of interlayer on the strength and deformation of layered rock specimens in uniaxial tests. In another study, Tran et al. [2] have employed DEM algorithm to simulate the behavior of concrete under triaxial loading. Xu et al. [20] have proposed a comparison between DEM simulation and experiments while investigating the mechanical behavior of sea ice. Lommen et al. [17] have studied the relationship between particle stiffness and bulk material behavior in a numerical simulation context. Furthermore, the combination of DEM and other numerical techniques has been performed by Dratt and Katterfeld [21]. The authors have combined DEM with Finite Element Method (FEM) for investigating the dynamic deformation of machine parts in contact with particle flow. Besides, Zhou et al. [22] have combined DEM with Computational Fluid Dynamics (CFD) for modeling granular flow in hydraulic conveyor. So far, studies involving DEM technique could strongly improve the investigation of mechanical properties of particulate systems by enabling an access to the local behavior in a granular media. Such numerical simulation technique could also save time and cost compared with complex experiments in the design and development of machinery involving particulate systems.

In this study, DEM model was developed for investigating the transmission of stress in granular media under the compression force. To this aim, the following steps were adopted as a methodology. First, a set of DEM parameters for the granular media was collected in the available literature, involving dimensional, gravimetric, mechanical, and interaction properties. Precisely, the DEM parameters were the size distribution, shape, mass density, Young's modulus, Poisson's ratio, shear modulus, coefficient of static friction, coefficient of rolling friction and coefficient of restitution. In a second step, a compression test was designed and performed using DEM simulations. Simultaneously, local mechanical information of particles was recorded, including the stress, force chain transmission and so on. The obtained results allowed exploring the ability of DEM technique in a mechanical context. Moreover, the features of DEM method were exposed to monitoring and analyzing the displacements and forces of all particles in the considered granular media.

2. MATERIALS AND METHODS

2.1. Brief introduction to DEM

DEM was developed based on the simulation of the motion of separate particles in a granular medium [23]. Such motion is determined by solving Newton's translational and rotational equations of motion for individual particles. The translational equation of motion is given as below [24]

$$m_i \frac{dv_i}{dt} = \sum_j F_{ij} + m_i g, \quad (1)$$

where m_i is the mass of particle i , v_i is the velocity, t is the time, F_{ij} is the force of contact acting on the particle i from the particle j , and g is the gravity. The rotational equation of the motion is expressed as follow [23]

$$I_i \frac{d\omega_i}{dt} = \sum_j T_{ij}, \quad (2)$$

where I_i is the moment of inertia, ω_i is the angular velocity, and T_{ij} is the torque acting on the particle i from the particle j . In a DEM model, the contact force is commonly modeled by spring, dashpot, and frictional slider [25, 26]. One of the most used contact models is the Hertz–Mindlin model [27], involving various parameters such as Young's modulus, Poisson's ratio, shear modulus, coefficient of static friction, coefficient of rolling friction and coefficient of restitution [28]. These coefficients, relating the relationships between particle/particle and particle/wall, were introduced to characterize the loss of energy when the particles interact. Based on this principle, DEM simulation could reflect the interactions occurring inside the granular media [18]. Underlying assumptions of DEM model include isotropy and elasticity of the considered particles.

On the other hand, the spherical element is the fundamental element in a DEM model. The description of DEM model is well documented in Lommen et al. [17] and Xie et al. [19]. One of the first applications of DEM was carried out by Cundall and Strack for investigating the mechanics of rock and soil [1]. Recently, the fast growth of computational capacity makes it more and more practical to employ numerical methods for solving engineering problems [16]. To date, many works using DEM technique for investigating the mechanical properties of granular materials have been published [2, 20, 29–31].

2.2. Description of compression test

The compression test used in this study is schematized in Fig. 1. Granular material with characteristics introduced in Tab. 1 was filled into a box container of $400 \times 100 \times 300$ mm. The initial height of the granular medium was 280 mm, exhibiting more than 47,000 particles. At the top of the container, a compression plate is placed. The latter can move freely along the vertical direction (z -axis). A confinement force is exerted to the compression plate, which compresses the granular medium uniformly under a constant loading. Such compression force is a constant normal one applying to the particles,

whereas the force acting on the upper part in the x -direction is perpendicular to the normal force, which was previously mentioned. Such a design of the test allows characterizing the transmission of force in the granular medium locally, under compression using a numerical DEM approach.

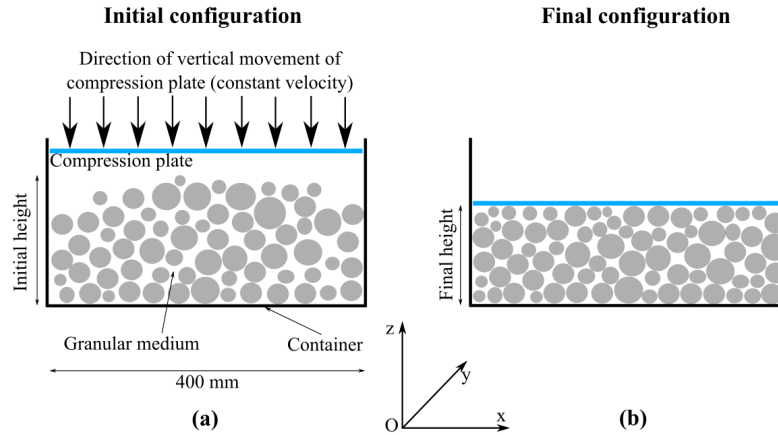


Fig. 1. Design of compression test in this study

2.3. DEM input parameters

In this study, the mechanical behavior of agricultural granular materials was investigated, such as dry soybean grains (Glycine max variety, moisture content lower than 10%) to develop and design the seeding machine. The microscopic parameters of soybean particles are commonly represented based on four categories, as in the following.

The first category includes gravimetric properties such as the true density. The second category includes dimensional properties, especially size (i.e., equivalent diameter) and shape. The third category includes mechanical properties, such as shear modulus, Young's modulus, and Poisson's ratio. The last category includes the interaction properties, such as friction (coefficient of static friction particle/particle and particle/wall, coefficient of rolling friction particle/particle and particle/wall), restitution (coefficient of restitution particle/particle, and particle/wall). It should be noticed that the calibration of all microscopic parameters for soybean grains is not an easy task [32]. Thus, in this study, the microscopic parameters (i.e., DEM input parameters) of particles were taken from the available literature of Ghodki et al. [32], as it was reported for the same variety of soybean. Moreover, Ghodki et al. [32] have admitted a single sphere modeling for the shape of particles, which allowed reducing the computational time considerably compared to multi-spheres or superquadric approaches [33]. It should be noticed that such single sphere modeling was selected based on the shape characterization of the considered particles [32].

In this study, the LIGGGHTS® code (stand for Open Source Discrete Element Method Particle Simulation) was used for the DEM simulations [34]. A no-cohesion nonlinear Hertz–Mindlin model was used for simulating the contact between particle-particle and

particle-wall, as recommended by various works, such as Raji et al. [25], or Horabik et al. [35]. Tab. 1 indicates the details of DEM simulation performed in this study, including the DEM input parameters collected from the available literature [32]. The simulations

Table 1. Parameters of DEM simulations in this study

Parameter	Description and value	Unit
Contact model	Sliding friction: Hertz-Mindlin	
	Rolling friction: constant directional torque	
	Cohesion: none	
Gravity	9.81	m/s ²
Particle shape model	Spherical	
Time step	1e-5	s
Particle size	6.24	mm
True density of particles	1220	kg/m ³
Young's modulus of particles	50	MPa
Poisson's ratio of particles	0.26	
Shear modulus of particles	19.84	MPa
Young's modulus of wall	3000	MPa
Poisson's ratio of wall	0.37	
Shear modulus of wall	1095	MPa
Coefficient of static friction particle/particle	0.26	
Coefficient of static friction particle/wall	0.30	
Coefficient of restitution particle/particle	0.17	
Coefficient of restitution particle/wall	0.35	
Coefficient of rolling friction particle/particle	0.08	
Coefficient of rolling friction particle/wall	0.08	
Length of container	400	mm
Width of container	100	mm
Number of particles	47362	
Initial fill height	280	mm
Final height	200	mm
Mesh of wall	Triangular type (STL)	
Number of elements (container and plate)	15604	
Element area	Average: 7.06e-5	m ²
Minimum angle	Average: 54.15	°
Aspect ratio	Average: 1.05	
Velocity of compression plate	10 ⁻¹	m/s

were performed using a Lenovo ThinkPad L420 Intel Core i5-2520M 2.50 GHz, 8 Gb of RAM, whereas the post-treatments were performed by using Matlab R2018a [36] and Paraview 5.4.1 [37].

In order to ensure the relevance of the selected set of DEM input parameters, indicated in Tab. 1, size characterization and silo discharge tests were performed. More precisely, the size characterization allowed obtaining a particle size distribution of particles (for generating particle diameter in DEM simulations), whereas the silo discharge test allowed checking the efficiency of friction coefficients (i.e., static and rolling frictions particle/particle). Brief details of these two investigations are following.

The size characterization of particles was conducted using a home-made imaging platform (4.42 MP/cm² pixel density Fujifilm X-E2S camera with a Fujinon XF18-55mm F2.8-4 R LM OIS lens), allowed obtaining an image resolution of 16 pixels per mm (recommended for characterizing particles greater than 3 mm in size [38]). Soybean grains were randomly selected for capturing images (about 900 grains were tested). Fig. 2(a) shows the raw image, whereas Fig. 2(b) presents the processed binary image indicating the equivalent diameter of each particle. The equivalent diameter was computed based on the obtained area of the particle. Using 900 equivalent diameters, the particle size distribution is shown in Fig. 2(c), exhibiting an average of 6.33 mm and a standard deviation of 0.46 mm. It is seen that the average particle diameter obtained by image analysis in this study was very close to the result obtained by Ghodki et al. [32] for the same soybean variety (i.e., 6.24 mm). Finally, the particle size distribution was used for generating particle diameter in DEM simulations.

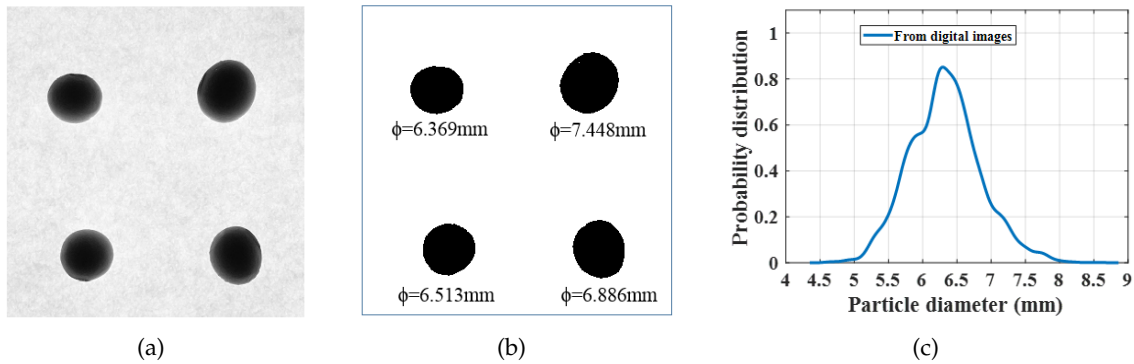


Fig. 2. Size characterization of particles in this study: (a) raw image, (b) processed image with an equivalent diameter of each particle, and (c) particle size distribution from image analysis

Regarding the discharge test, a flat-bottomed rectangular silo of 160 and 100 mm of length and width, respectively, together with a circular orifice of 50 mm of diameter, was prepared. A kg of soybean particles was randomly selected and filled into the silo, exhibiting a fill height of 100 mm. In the DEM simulation, the same procedure was applied. As friction plays the most critical role in the rheology behavior of granular materials [39], the efficiency of the selected coefficients of static and rolling frictions particle/particle

(see Tab. 1) were checked based on this test. To this aim, in DEM simulation, the coefficient of static friction was varied in a 0.18–0.34 range with a step of 0.04, whereas the coefficient of rolling friction was varied between 0.05–0.14 with a step of 0.03. A macroscopic property, the final mass retained in the silo after discharged, was chosen to make comparisons between experiment and DEM simulations.

3. RESULTS AND DISCUSSIONS

3.1. Validation of numerical model

In this section, the numerical DEM model is compared with experimental work in the literature to evaluate the effectiveness of the model. Fig. 3(a) presents the initial assembly of particles in the box container, described in Section 2.2, whereas Fig. 3(b) shows the initial force chain network of the medium, as well as a visualization of the compression plate and its triangular mesh.

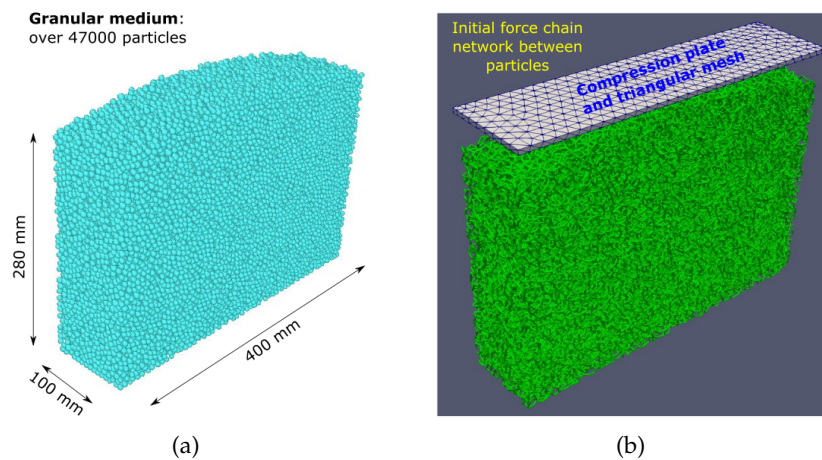


Fig. 3. Visualization of: (a) particle assembly at initial configuration and (b) initial force chain network and compression plate with triangular mesh

As recommended by various works in the literature [10, 40], the coefficient of static friction particle/particle is characterized by the ratio of the shear stress to the normal stress, while the granular material is subjected to loading. In this case of compression, the stresses in the x -axis (tangential to the direction of compression) and z -axis (normal to the direction of compression) were calculated by the corresponding wall reaction forces. More precisely, such reactions were calculated based on the reaction forces in each triangular mesh element in contact with particles [40]. Figs. 4(a) and 4(b) show the evolution of normal stress and shear stress over elapsed time. The comparison between the shear stress to normal stress ratio and the work of Ghodki et al. [32] for the considered granular material is shown in Fig. 4(c). In Ghodki et al. [32], the inter-particle friction coefficient of 0.26 was calibrated by combining the experimental angle of repose test and DEM simulation (calibration result was indicated in Section 3.2 in Ghodki et al. [32]). As can be seen

in Fig. 4(c), the normal stress on the wall starts to increase when the compression plate contacts with the particle assembly. A small overshoot is also observed, due to the first interactions between particles and compression plate. The compression plate is vertically moved in order to compress the granular material under constant velocity. As for discrete elements, the particles arranged in order to respond to the loading. Finally, the granular medium reaches a convergence in both the normal and shear stress. Such convergence exhibits the equilibrium of the granular medium under constant loading. As shown in Fig. 4(c), the ratio of shear stress to normal stress at equilibrium state under constant loading is highly correlated compared with the work of Ghodki et al. [32] for the considered granular material, showing a high effectiveness of the proposed numerical DEM model.

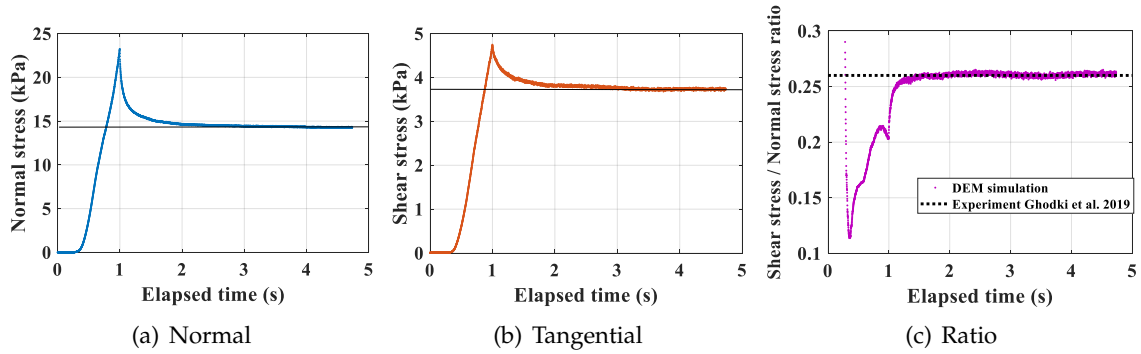


Fig. 4. Evaluation of: (a) normal stress, (b) shear stress, and (c) shear stress/normal stress ratio over time

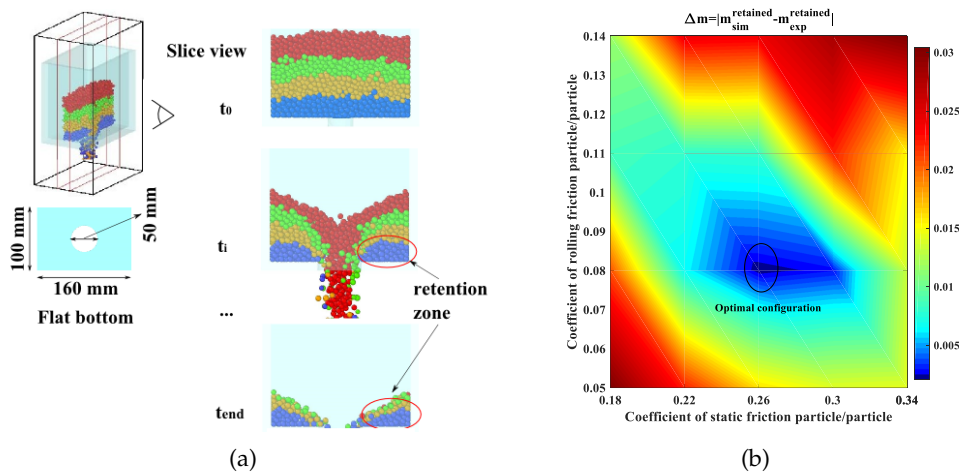


Fig. 5. Results of silo discharge test: (a) visualization of particle flow at different colored layers and retention zone, (b) evolution of Δm in function of the coefficient of static friction particle/particle and coefficient of rolling friction particle/particle

In addition, the results of the silo discharge test are presented in Fig. 5. Visualization of discharge flow at different colored layers in a slice view mode is presented in Fig. 5(a), showing the retention zone in the flat-bottomed silo. Fig. 5(b) shows the difference Δm between mass retained in the silo from DEM simulations and experiment, in function of the friction coefficients particle/particle. It is shown that the difference Δm could vary between 2 and 30 g. The mass retained in the experiment was 176.7 g. It is seen that the couple of (0.26, 0.08) allowed obtaining the smallest value of Δm (2.1 g). Thus, the efficiency of the selected friction coefficients was confirmed, allowed having more confident results.

3.2. Investigation of transmission of force

In this section, the numerical DEM model was used to investigate the transmission of force in the granular medium under compression. Fig. 6 shows the evolution of particle velocity (z-velocity, x-velocity, and velocity magnitude, respectively) at different positions of the compression plate. Fig. 7 presents the corresponding configurations of the granular medium, including the force chain network (z-direction, x-direction, and force magnitude, respectively). It is seen that the most moving particles are those in contact with the compression plate. As the compression plate was moved in the z-direction, the velocity in z-direction was dominant compared to other directions.

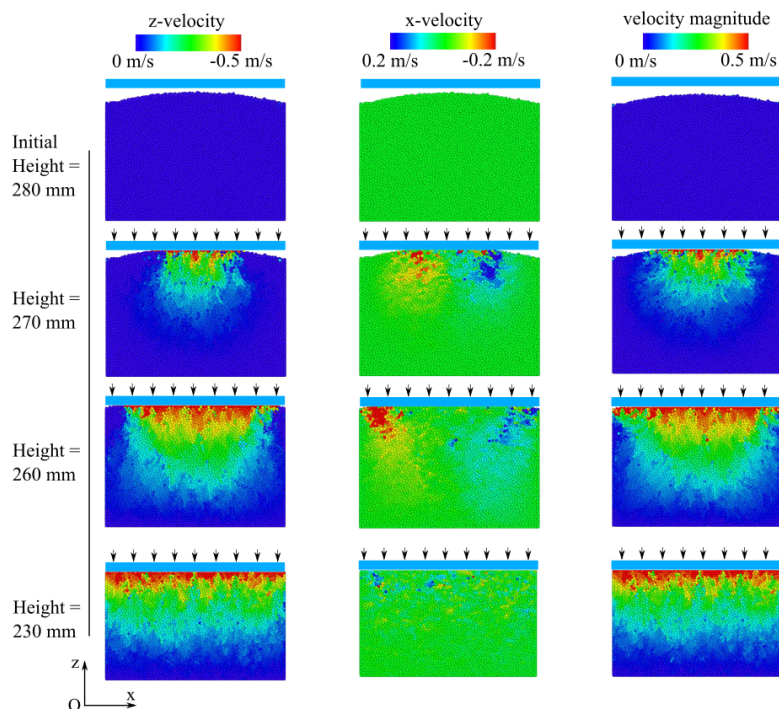


Fig. 6. Visualization of the velocity field of particles in the granular medium at different positions of the compression plate. The colorbar was adapted for each velocity field in order to explore the most appropriate vision effect

Regarding the force chain network (Fig. 7), at initial configuration (without loading from compression plate), the force chains with low amplitude were created at the bottom of the granular medium, showing the influence of the weight of particles at the top level. However, at initial configuration, the force chains generally had no specific orientations, i.e., the contact forces were uniformly distributed in the medium. When the compression plate contacts with the medium at heights of 270, 260, and 230 mm, the force chains were progressively created, also in increasing amplitude. The contact forces in the z -direction were significant compared to those in the x -direction. This is also proved when regarding the velocity field (Fig. 6). This exciting result showed how the compression forces were transmitted through the particulate system. The orientations of force chains are mainly parallel to the vertical axis, which is the direction of the compression loading. The transmission network also provides information on the structural arrangement, related to the change of the microstructure to respond to the loading.

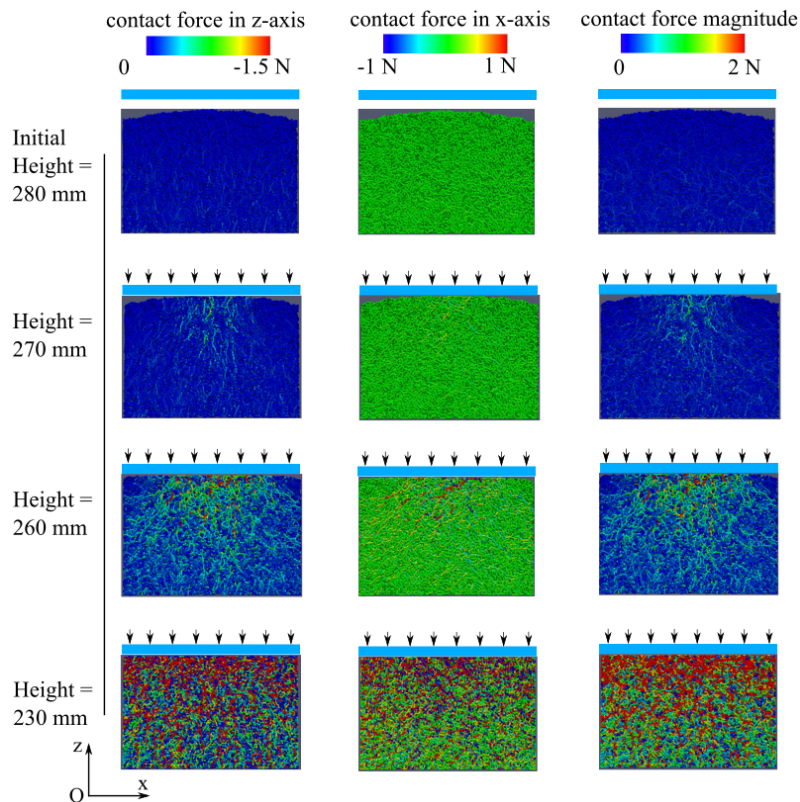


Fig. 7. Visualization of force chain network in the granular medium at different positions of compression plate. The colorbar was adapted for each case in order to explore the most appropriate vision effect

Fig. 8(a) presents the increase of number of contact forces in function of fill height, normalized to the number of contact force at initial configuration (i.e., 100%), whereas Fig. 8(b) shows the evolution of the number of contact forces in function of elapsed time.

It is seen that the number of contact forces linearly increased, as expected, because of the uniform movement of the compression plate. At the equilibrium state, the number of contact forces was increased by about 170% and remained a horizontal asymptotic, as seen in Fig. 8(b). The average and standard deviation values of the probability density distribution of the force chain network are also presented in Fig. 9(a), and 9(b), respectively, in function of fill height. As the compression is in the z-direction, the mean value of the contact force in the z-direction was the highest. However, contact forces exhibit approximately the similar standard deviation values in all the directions. Finally, Fig. 9(c) presents the statistical distribution of the magnitude of contact forces, including their average and standard deviation. Statistically, the contact forces increase in both amplitude and standard deviation.

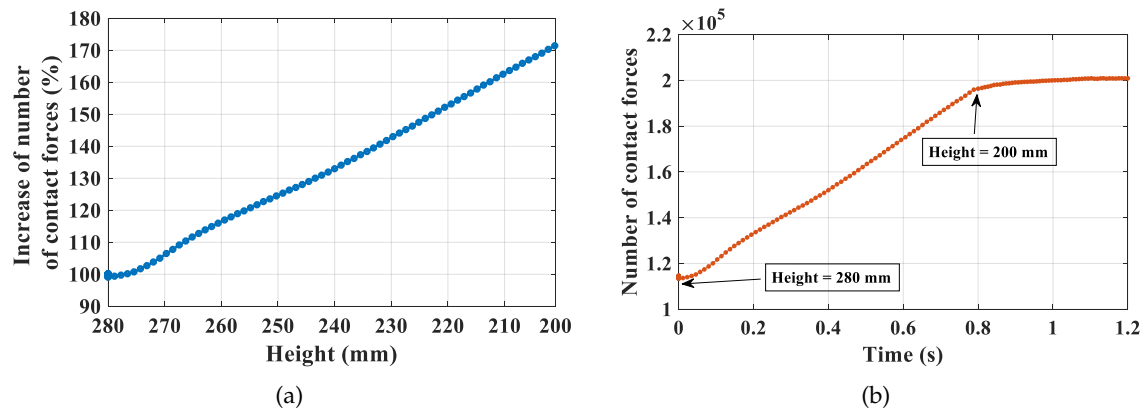


Fig. 8. Evaluation of the number of contact forces in function of (a) fill height and (b) elapsed time

The force vectors presented in Fig. 9 were employed to calculate the total force exerted on each particle in the system. At the maximum compression point of 200 mm of height, Fig. 10(a) presents the histogram of the number of particles in contact with a given particle, whereas the histogram of total force exerted on all the particles is shown in Fig. 10(b). The total force exerted on a given particle was calculated by the sum of all the contact forces of its surrounding particles. It can be noticed that at the maximum compression point of 200 mm, each particle was exposed to an average of 8 surrounding particles, whereas the average of total force exerted was 33 N, with a standard deviation of about 13 N.

In Appendix, the measurement of the critical breakage force that causes the soybean grains to crack is presented. Results showed that the critical compressive force was in the range of 50-70 N (approximately 1.5 mm of particle deformation). Based on the results obtained (Fig. 10(b)) and the measurement of breakage force, it can be seen that the 200 mm compression point was a critical limit for maintaining the bond between particles. If the compression increased further, the total force exerted on particles would also increase, leading to the destruction of particle bonds.

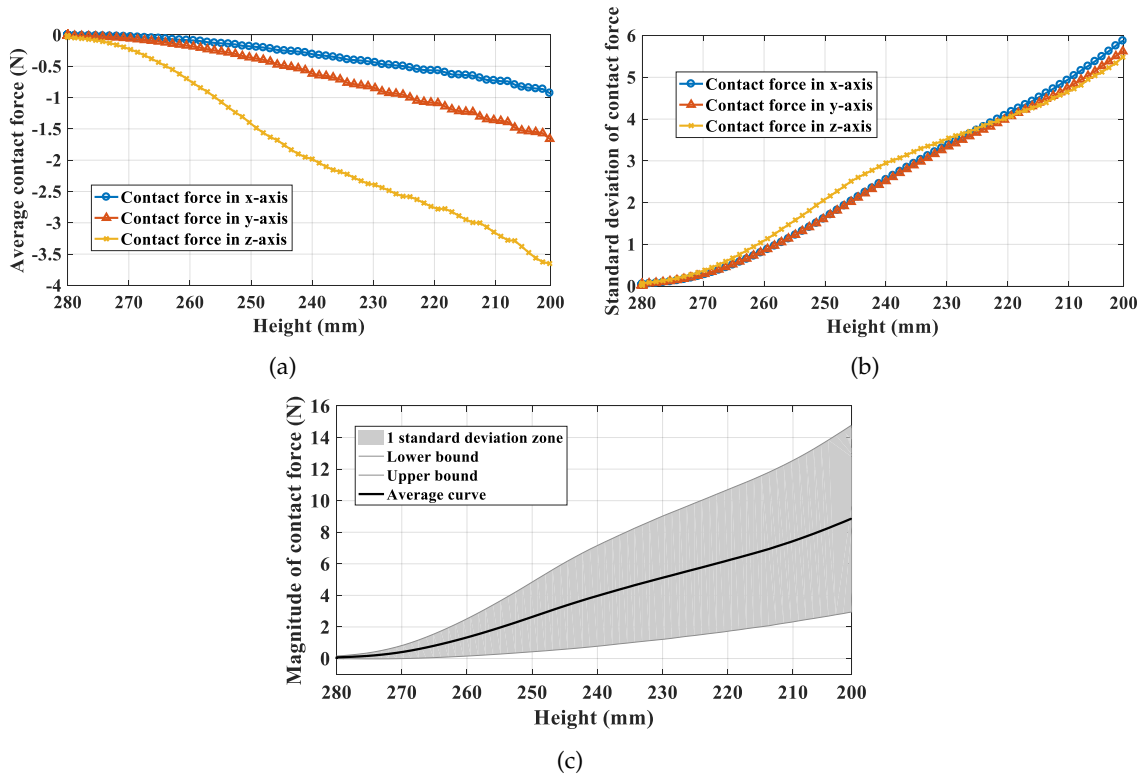


Fig. 9. Evaluation of contact force at different fill heights: (a) average value, (b) standard deviation value, and (c) contact force magnitude

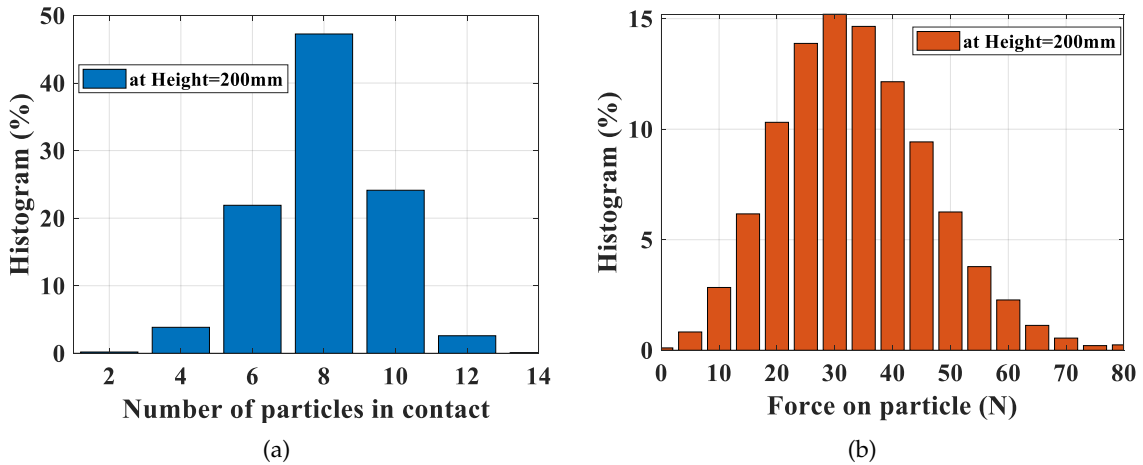


Fig. 10. Evaluation of contact force at Height = 200 mm: (a) number of particles in contact, (b) distribution of total force exerted on particles

3.3. Discussions

The main findings of this work could be summarized as the followings:

- A calibration procedure of a numerical DEM model for a granular assembly was presented and validated with experimental data;
- The DEM model was developed, allowed investigating the transmission of force in the granular medium under compression loading;
- The force chain network was statistically quantified, showing the response of the granular medium under loading.

Indeed, for a given granular medium under loading, the force chain network could be considered as a load-bearing system [41]. The force chain network allows the granular material to adapt itself in order to support different loadings and boundary conditions. From a material point of view, the force chain network characterizes the microstructure of the granular material. It has been pointed out that the granular material can change its microstructure in order to bear the given loadings [42]. Moreover, the weak network of particles surrounds the force chain network has been reported as the principal energy dissipation source by various works in the literature [43]. Therefore, the results of this study confirm the role of the force chain network in granular mechanics as such network governs the mechanical response of the materials.

In order to explore the influence of microscopic particle parameters on the force chain network, especially from friction point of view, DEM simulation for compression test was repeated in changing the value of the coefficient of static friction particle/particle and coefficient of rolling friction particle/particle, respectively. The results of such a sensitivity analysis are presented in Fig. 11. Figs. 11(a) and 11(b) show the deviation of the number and magnitude of contact forces in function of the deviation of coefficient of static friction particle/particle, respectively (coefficient of static friction particle/particle varied in the range of [0.20, 0.26 and 0.32]). On the other hand, Figs. 11(c) and 11(d) show the deviation of the number and magnitude of contact forces in function of the deviation of the coefficient of rolling friction particle/particle, respectively (coefficient of rolling friction particle/particle varied in the range of [0.05, 0.08 and 0.11]). It could be observed that changing the value of microscopic parameters of particles modified the force chain network in terms of both number and magnitude of contact forces, with different amplitudes at different heights. A higher friction coefficient allowed obtaining a more significant number and magnitude of contact forces, which was also observed in different studies in the literature [44, 45]. Besides, it can be seen that the coefficient of static friction particle/particle exhibited a more critical role than the rolling friction coefficient in the compression problem, especially in terms of the magnitude of contact forces. The reason is that the rolling resistance is mainly considered in dynamic impact problems, as pointed out by Zhang et al. [46].

Certainly, further investigations should be carried out in order to explore the failure of the granular materials, i.e., buckling of force chains. Such an investigation could indicate the stability of the force chain network and which parameters that the stability depends on. On the other hand, the relationship between the force chain network and the energy of the particulate system should also be examined to clarify the energy

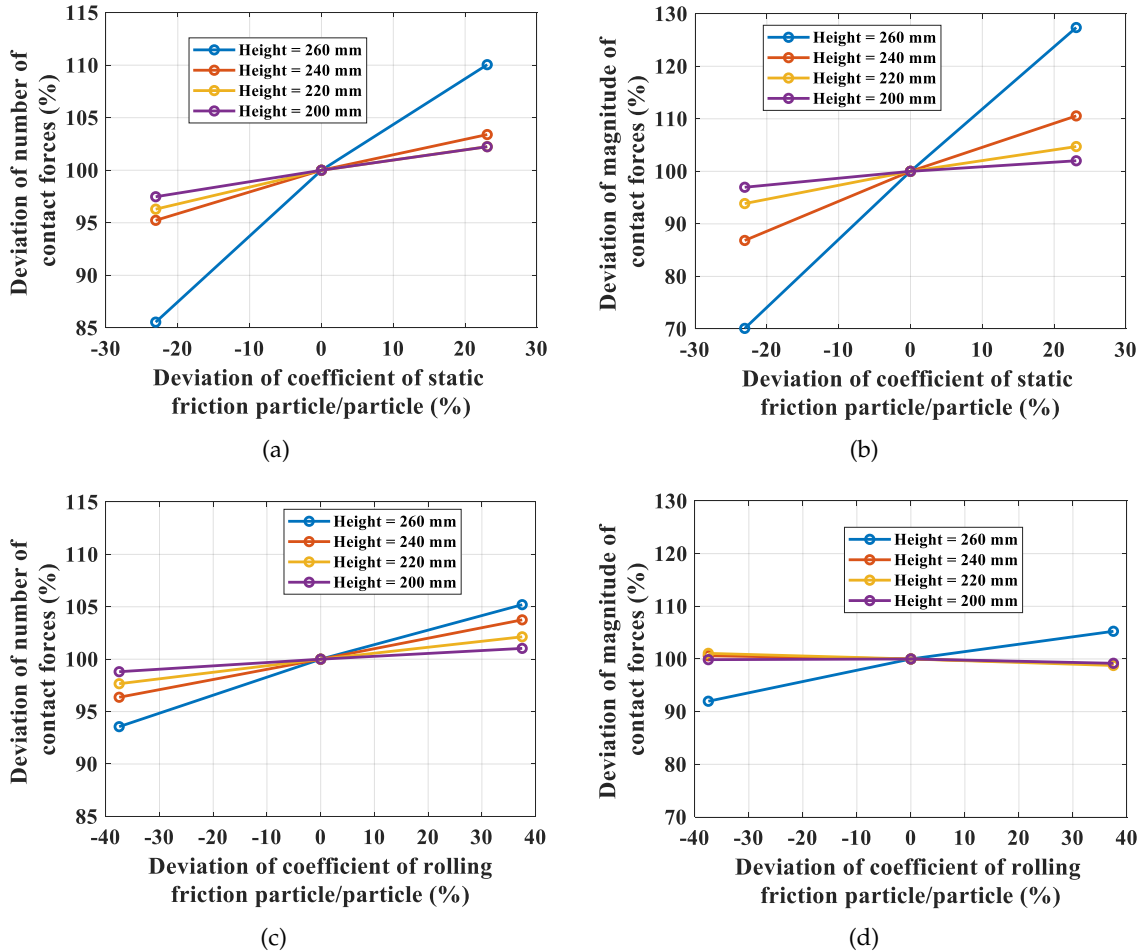


Fig. 11. Evaluation of the number of contact forces in function of: (a) coefficient of static friction particle/particle, (c) coefficient of rolling friction particle/particle; evaluation of the magnitude of contact forces in function of: (b) the coefficient of static friction particle/particle, (d) coefficient of rolling friction particle/particle

dissipation. Finally, more complex mechanical tests should be conducted, which could establish the relationship between the microscale parameters and macroscopic responses of the granular media.

4. CONCLUSIONS

In this work, numerical simulation of the compression test for a granular medium has been presented to investigate the force transmission. The numerical DEM model was calibrated, taking into account the microscale parameters of the granular medium, especially the particle size distribution, mechanical properties, coefficient of static friction, coefficient of rolling friction and coefficient of restitution. The DEM model was

compared with experimental data, showing a good capability of simulation. The force chain network of the granular medium was calculated, showing the crucial role of such a network on the macroscopic mechanical response of the medium. Contact forces were analyzed statistically, presenting its evaluation in function of the applied load. Results showed that the more the compression applied, the higher number of contacts forces was created, along with an increase of amplitude and standard deviation. In addition, further works should be conducted and applied for different granular materials and also under different loading conditions. Moving walls with constant lateral confinement should be investigated in further studies as they can affect the settlement of the sample in the z -direction and the static/dynamic states of the sample at the time step. Finally, the failure of granular materials should be investigated regarding the collapse of the force chain network at the micro-level.

ACKNOWLEDGMENT

The authors gratefully acknowledge the Vietnam National University of Agriculture for supporting this research.

REFERENCES

- [1] P. A. Cundall and O. D. L. Strack. A discrete numerical model for granular assemblies. *Geotechnique*, **29**, (1), (1979), pp. 47–65. <https://doi.org/10.1680/geot.1979.29.1.47>.
- [2] V. T. Tran, F.-V. Donzé, and P. Marin. A discrete element model of concrete under high triaxial loading. *Cement and Concrete Composites*, **33**, (9), (2011), pp. 936–948. <https://doi.org/10.1016/j.cemconcomp.2011.01.003>.
- [3] Z. Kaliniewicz and Z. Żuk. A relationship between friction plate roughness and the external friction angle of wheat kernels. *International Journal of Food Properties*, **20**, (sup3), (2017), pp. S2409–S2417. <https://doi.org/10.1080/10942912.2017.1371190>.
- [4] N. T. Cuong, B. H. Ha, and R. Fukagawa. Failure mechanism of two-dimensional granular columns: Numerical simulation and experiments. *Vietnam Journal of Mechanics*, **37**, (4), (2015), pp. 239–250. <https://doi.org/10.15625/0866-7136/37/4/5844>.
- [5] H. Fu, C. Jin, and J. Yu. The DEM-based digital design platform for agricultural machinery—AgriDEM. In *International Conference on Discrete Element Methods*, Springer, Springer, (2016), pp. 1253–1263.
- [6] J. Horabik and M. Molenda. Force and contact area of wheat grain in friction. *Journal of Agricultural Engineering Research*, **41**, (1), (1988), pp. 33–42. [https://doi.org/10.1016/0021-8634\(88\)90201-6](https://doi.org/10.1016/0021-8634(88)90201-6).
- [7] E. P. Montellà, M. Toraldo, B. Chareyre, and L. Sibille. Localized fluidization in granular materials: Theoretical and numerical study. *Physical Review E*, **94**, (5), (2016). <https://doi.org/10.1103/physreve.94.052905>.
- [8] D. T. Huan, T. H. Quoc, and T. M. Tu. Free vibration analysis of functionally graded shell panels with various geometric shapes in thermal environment. *Vietnam Journal of Mechanics*, **40**, (3), (2018), pp. 199–215. <https://doi.org/10.15625/0866-7136/10776>.
- [9] F. Nicot, H. Xiong, A. Wautier, J. Lerbet, and F. Darve. Force chain collapse as grain column buckling in granular materials. *Granular Matter*, **19**, (2), (2017). <https://doi.org/10.1007/s10035-017-0702-0>.

- [10] Y. Zhou, H. Wang, B. Zhou, and J. Li. DEM-aided direct shear testing of granular sands incorporating realistic particle shape. *Granular Matter*, **20**, (3), (2018). <https://doi.org/10.1007/s10035-018-0828-8>.
- [11] Z. Deng, P. B. Umbanhowar, J. M. Ottino, and R. M. Lueptow. Continuum modelling of segregating tridisperse granular chute flow. *Proceedings of the Royal Society A: Mathematical, Physical and Engineering Sciences*, **474**, (2211), (2018). <https://doi.org/10.1098/rspa.2017.0384>.
- [12] S. Dunatunga and K. Kamrin. Continuum modelling and simulation of granular flows through their many phases. *Journal of Fluid Mechanics*, **779**, (2015), pp. 483–513. <https://doi.org/10.1017/jfm.2015.383>.
- [13] S. Bidier and W. Ehlers. Particle simulation of granular media and homogenisation towards continuum quantities. *PAMM*, **13**, (1), (2013), pp. 575–576. <https://doi.org/10.1002/pamm.201310269>.
- [14] M. Tolomeo, V. Richefeu, G. Combe, J. N. Roux, and G. Viggiani. An assessment of discrete element approaches to infer intergranular forces from experiments on 2D granular media. *International Journal of Solids and Structures*, **187**, (2020), pp. 48–57. <https://doi.org/10.1016/j.ijsolstr.2019.01.010>.
- [15] J. Duriez and R. Wan. Stress in wet granular media with interfaces via homogenization and discrete element approaches. *Journal of Engineering Mechanics*, **142**, (12), (2016). [https://doi.org/10.1061/\(asce\)em.1943-7889.0001163](https://doi.org/10.1061/(asce)em.1943-7889.0001163).
- [16] M. Servin, D. Wang, C. Lacoursière, and K. Bodin. Examining the smooth and nonsmooth discrete element approaches to granular matter. *International Journal for Numerical Methods in Engineering*, **97**, (12), (2014), pp. 878–902. <https://doi.org/10.1002/nme.4612>.
- [17] S. Lommen, D. Schott, and G. Lodewijks. DEM speedup: Stiffness effects on behavior of bulk material. *Particuology*, **12**, (2014), pp. 107–112. <https://doi.org/10.1016/j.partic.2013.03.006>.
- [18] V. D. Than, S. Khamseh, A. M. Tang, J.-M. Pereira, F. Chevoir, and J.-N. Roux. Basic mechanical properties of wet granular materials: a DEM study. *Journal of Engineering Mechanics*, **143**, (1), (2017). [https://doi.org/10.1061/\(asce\)em.1943-7889.0001043](https://doi.org/10.1061/(asce)em.1943-7889.0001043).
- [19] L. Xie, P. Jin, T.-C. Su, X. Li, and Z. Liang. Numerical simulation of uniaxial compression tests on layered rock specimens using the discrete element method. *Computational Particle Mechanics*, (2019), pp. 1–10. <https://doi.org/10.1007/s40571-019-00307-3>.
- [20] Z. Xu, A. M. Tartakovsky, and W. Pan. Discrete-element model for the interaction between ocean waves and sea ice. *Physical Review E*, **85**, (1), (2012). <https://doi.org/10.1103/physreve.85.016703>.
- [21] M. Dratt and A. Katterfeld. Coupling of FEM and DEM simulations to consider dynamic deformations under particle load. *Granular Matter*, **19**, (3), (2017). <https://doi.org/10.1007/s10035-017-0728-3>.
- [22] M. Zhou, S. Wang, S. Kuang, K. Luo, J. Fan, and A. Yu. CFD-DEM modelling of hydraulic conveying of solid particles in a vertical pipe. *Powder Technology*, **354**, (2019), pp. 893–905. <https://doi.org/10.1016/j.powtec.2019.07.015>.
- [23] M. Kobayakawa, S. Miyai, T. Tsuji, and T. Tanaka. Interaction between dry granular materials and an inclined plate (comparison between large-scale DEM simulation and three-dimensional wedge model). *Journal of Terramechanics*, (2019). <https://doi.org/10.1016/j.jterra.2019.08.006>.
- [24] C. González-Montellano, J. M. Fuentes, E. Ayuga-Téllez, and F. Ayuga. Determination of the mechanical properties of maize grains and olives required for use in DEM simulations. *Journal of Food Engineering*, **111**, (4), (2012), pp. 553–562. <https://doi.org/10.1016/j.jfoodeng.2012.03.017>.

- [25] A. O. Raji and J. F. Favier. Model for the deformation in agricultural and food particulate materials under bulk compressive loading using discrete element method. I: Theory, model development and validation. *Journal of Food Engineering*, **64**, (3), (2004), pp. 359–371. <https://doi.org/10.1016/j.jfoodeng.2003.11.004>.
- [26] V.-T. Nguyen and M.-Q. Le. Atomistic simulation of the uniaxial compression of black phosphorene nanotubes. *Vietnam Journal of Mechanics*, **40**, (3), (2018), pp. 243–250. <https://doi.org/10.15625/0866-7136/10982>.
- [27] K. L. Johnson, K. Kendall, and a. Roberts. Surface energy and the contact of elastic solids. In *Proceedings of the Royal Society of London. Series A. Mathematical and Physical Sciences*, The Royal Society London, Vol. 324, (1971), pp. 301–313, <https://doi.org/10.1098/rspa.1971.0141>.
- [28] A. Di Renzo and F. P. Di Maio. Comparison of contact-force models for the simulation of collisions in DEM-based granular flow codes. *Chemical Engineering Science*, **59**, (3), (2004), pp. 525–541. <https://doi.org/10.1016/j.ces.2003.09.037>.
- [29] K. F. Malone and B. H. Xu. Determination of contact parameters for discrete element method simulations of granular systems. *Particuology*, **6**, (6), (2008), pp. 521–528. <https://doi.org/10.1016/j.partic.2008.07.012>.
- [30] J. Ai, J.-F. Chen, J. M. Rotter, and J. Y. Ooi. Assessment of rolling resistance models in discrete element simulations. *Powder Technology*, **206**, (3), (2011), pp. 269–282. <https://doi.org/10.1016/j.powtec.2010.09.030>.
- [31] J. M. Boac, R. P. K. Ambrose, M. E. Casada, R. G. Maghirang, and D. E. Maier. Applications of discrete element method in modeling of grain postharvest operations. *Food Engineering Reviews*, **6**, (4), (2014), pp. 128–149. <https://doi.org/10.1007/s12393-014-9090-y>.
- [32] B. M. Ghodki, M. Patel, R. Namdeo, and G. Carpenter. Calibration of discrete element model parameters: soybeans. *Computational Particle Mechanics*, **6**, (1), (2019), pp. 3–10. <https://doi.org/10.1007/s40571-018-0194-7>.
- [33] T. Xu, J. Yu, Y. Yu, and Y. Wang. A modelling and verification approach for soybean seed particles using the discrete element method. *Advanced Powder Technology*, **29**, (12), (2018), pp. 3274–3290. <https://doi.org/10.1016/j.appt.2018.09.006>.
- [34] C. Kloss, C. Goniva, A. Hager, S. Amberger, and S. Pirker. Models, algorithms and validation for opensource DEM and CFD-DEM. *Progress in Computational Fluid Dynamics, an International Journal*, **12**, (2-3), (2012), pp. 140–152. <https://doi.org/10.1504/pcfd.2012.047457>.
- [35] J. Horabik and M. Molenda. Parameters and contact models for DEM simulations of agricultural granular materials: A review. *Biosystems Engineering*, **147**, (2016), pp. 206–225. <https://doi.org/10.1016/j.biosystemseng.2016.02.017>.
- [36] *Matlab*. Natick, MA, USA, (2018). The MathWorks.
- [37] U. Ayachit. *The ParaView guide: A parallel visualization application*, ParaView 4.3. Kitware, Incorporated, (2015).
- [38] D. O. C. Souza and F. C. Menegalli. Image analysis: Statistical study of particle size distribution and shape characterization. *Powder Technology*, **214**, (1), (2011), pp. 57–63. <https://doi.org/10.1016/j.powtec.2011.07.035>.
- [39] C. J. Coetzee and D. N. J. Els. Calibration of granular material parameters for DEM modelling and numerical verification by blade–granular material interaction. *Journal of Terramechanics*, **46**, (1), (2009), pp. 15–26. <https://doi.org/10.1016/j.jterra.2008.12.004>.
- [40] T. A. H. Simons, R. Weiler, S. Strege, S. Bensmann, M. Schilling, and A. Kwade. A ring shear tester as calibration experiment for DEM simulations in agitated mixers—a sensitivity study. *Procedia Engineering*, **102**, (1), (2015), pp. 741–748. <https://doi.org/10.1016/j.proeng.2015.01.178>.

- [41] W. Wu, G. Ma, W. Zhou, D. Wang, and X. Chang. Force transmission and anisotropic characteristics of sheared granular materials with rolling resistance. *Granular Matter*, **21**, (4), (2019). <https://doi.org/10.1007/s10035-019-0938-y>.
- [42] A. Salazar, E. Sáez, and G. Pardo. Modeling the direct shear test of a coarse sand using the 3D Discrete Element Method with a rolling friction model. *Computers and Geotechnics*, **67**, (2015), pp. 83–93. <https://doi.org/10.1016/j.compgeo.2015.02.017>.
- [43] A. Tordesillas, C. A. H. Steer, and D. M. Walker. Force chain and contact cycle evolution in a dense granular material under shallow penetration. *Nonlinear Processes in Geophysics*, **21**, (2), (2014), pp. 505–519. <https://doi.org/10.5194/npg-21-505-2014>.
- [44] T.-X. Xiu, W. Wang, K. Liu, Z.-Y. Wang, and D.-Z. Wei. Characteristics of force chains in frictional interface during abrasive flow machining based on discrete element method. *Advances in Manufacturing*, **6**, (4), (2018), pp. 355–375. <https://doi.org/10.1007/s40436-018-0236-7>.
- [45] W. Wang, W. Gu, and K. Liu. Force chain evolution and force characteristics of shearing granular media in Taylor-Couette geometry by DEM. *Tribology Transactions*, **58**, (2), (2015), pp. 197–206. <https://doi.org/10.1080/10402004.2014.943829>.
- [46] L. Zhang, N. G. H. Nguyen, S. Lambert, F. Nicot, F. Prunier, and I. Djeran-Maigre. The role of force chains in granular materials: from statics to dynamics. *European Journal of Environmental and Civil Engineering*, **21**, (7-8), (2017), pp. 874–895. <https://doi.org/10.1080/19648189.2016.1194332>.

APPENDIX

Critical breakage force

In this work, the critical breakage force of soybean particles was measured using F.S. 20,000 kN testing machine, available at the Strength of materials laboratory, Faculty of Engineering, Vietnam National University of Agriculture. In each test, three particles were positioned in the machine to form an equilateral triangle, as showing in Fig. A1(a). Three tests were finally conducted, as shown in Fig. A1(b) for displacement - compression force curves. The breakage of particles was observed at 50-70 N for most of the particles (i.e., a shortening higher than 1.5 mm compared to the average particle diameter of 6.24 mm). It should be noticed that the critical value should also be selected based on the germination rate of particles after being deformed (i.e., higher than 85-90%). Consequently, 50 N was finally chosen as a critical breakage force of soybean particles.

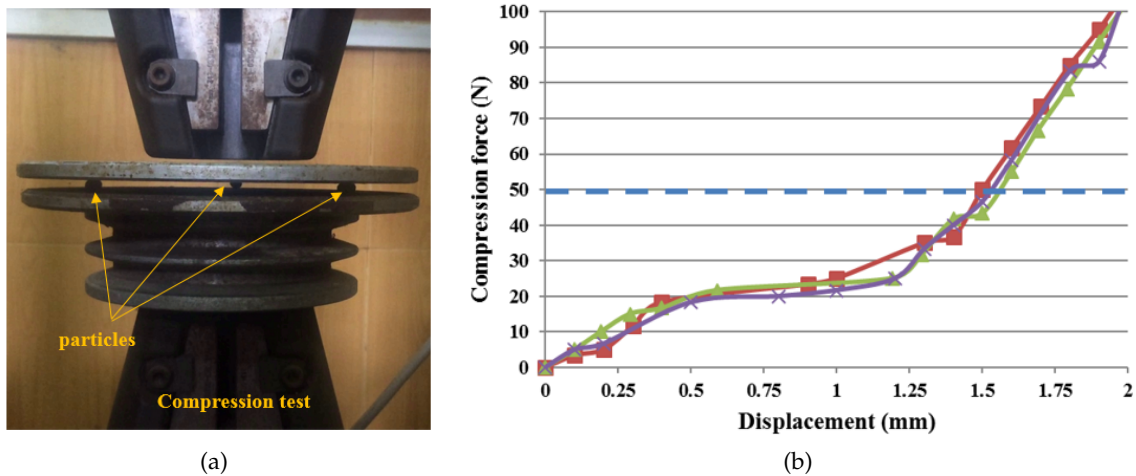


Fig. A1. Measurement of critical breakage force of particles: (a) compression test, (b) displacement - compression force curve